Article:
Jamwal, PK, Hussain, S, Tsoi, YH et al. (2017) Musculoskeletal modelling of human ankle complex: Estimation of ankle joint moments. Clinical Biomechanics, 44. pp. 75-82. ISSN: 0268-0033

https://doi.org/10.1016/j.clinbiomech.2017.03.010

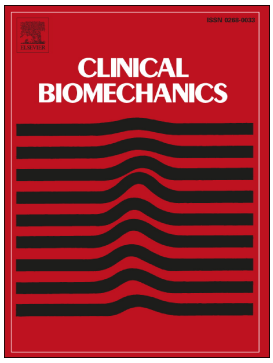

Musculoskeletal modelling of human ankle complex: Estimation of ankle joint moments

Prashant K. Jamwal, Shahid Hussain, Yun Ho Tsoi, Mergen H. Ghayesh, Sheng Quan Xie

PII: S0268-0033(17)30076-1
DOI: doi: 10.1016/j.clinbiomech.2017.03.010
Reference: JCLB 4306

To appear in: *Clinical Biomechanics*

Received date: 2 February 2016
Accepted date: 22 March 2017

Please cite this article as: Prashant K. Jamwal, Shahid Hussain, Yun Ho Tsoi, Mergen H. Ghayesh, Sheng Quan Xie , Musculoskeletal modelling of human ankle complex: Estimation of ankle joint moments. The address for the corresponding author was captured as affiliation for all authors. Please check if appropriate. Jclb(2017), doi: 10.1016/j.clinbiomech.2017.03.010

Word Count Abstract: 227
Word Count Main Text: 4328

Musculoskeletal Modelling of Human Ankle Complex: Estimation of Ankle Joint Moments

Prashant K. Jamwal[1], PhD, Shahid Hussain[2], PhD, Yun Ho Tsoi[3], PhD, Mergen H. Ghayesh[4], PhD and Sheng Quan Xie[5], PhD

[1]School of Electrical and Electronics Engineering, Nazarbayev University, Astana, Kazakhstan (prashant.jamwal@nu.edu.kz),
[2]School of Mechanical, Materials, Mechatronic and Biomedical Engineering, University of Wollongong, Wollongong, NSW, Australia (shussain@uow.edu.au),
[3]Rakon Limited, 8 Sylvia Park Road, Mt Wellington, Auckland, New Zealand (yunho.tsoi@gmail.com),
[4]School of Mechanical Engineering, University of Adelaide, Adelaide, SA, Australia (mergen.ghayesh@adelaide.edu.au),
[5]School of Electrical and Electronic Engineering and School of Mechanical Engineering, Faculty of Engineering, University of Leeds, Leeds, LS2, 9JT, UK
(s.q.xie@leeds.ac.uk)

***Abstract*—**

Background: A musculoskeletal model for the ankle complex is vital in order to enhance the understanding of neuro-mechanical control of ankle motions, diagnose ankle disorders and assess subsequent treatments. Motions at the human ankle and foot, however, are complex due to simultaneous movements at the two joints namely, the ankle joint and the subtalar joint. The musculoskeletal elements at the ankle complex, such as ligaments, muscles and tendons, have intricate arrangements and exhibit transient and nonlinear behaviour.

Methods: This paper develops a musculoskeletal model of the ankle complex considering the biaxial ankle structure. The model provides estimates of overall mechanical characteristics (motion and moments) of ankle complex through consideration of forces applied along ligaments and muscle-tendon units. The dynamics of the ankle complex and its surrounding ligaments and muscle-tendon units is modelled and formulated into a state space model to facilitate simulations. A graphical user interface is also developed during this research in order to include the visual anatomical information by converting it to quantitative information on coordinates.

Findings: Validation of the ankle model was carried out by comparing its outputs with those published in literature as well as with experimental data obtained from an existing parallel ankle rehabilitation robot.

Interpretation: Qualitative agreement was observed between the model and measured data for both, the passive and active ankle motions during trials in terms of displacements and moments.

***Keywords*—Ankle joint, musculoskeletal model, joint moments, parallel ankle robots.**

I. INTRODUCTION

UNDERSTANDING the mechanical properties of the human ankle musculoskeletal system is important for simulating human movements, in the study of multi-joint

mechanics, understanding neuro-mechanical control of human ankle, diagnosis and treatment of ankle disorders and assessment of subsequent treatments [1-3]. Ankle model can also provide important inputs during design and development of an ankle rehabilitation robot and assessment of various interaction control strategies implemented on the ankle robot [4, 5].

A comprehensive literature survey revealed that a range of computational ankle models with varying levels of complexities have been developed. Simpler models mainly involve treatment of the foot and lower limb as rigid bodies while other complex models typically utilise finite element analysis to study stresses and strains in the soft tissues [6-8], and three-dimensional contacts to describe the ankle kinematics [9]. While complex models are unsuitable for dynamic simulation, they also fail to provide forces along the ankle ligaments, which is important for the research on ankle joint rehabilitation.

Kinematics of the ankle complex has been studied in the past [10, 11] and while some models describe its motion as purely rotational [12-15], others consider foot motions to be a consequence of rotations about two hinge/revolute joints (biaxial) in series [16, 17] [18-24]. Ankle complex kinematics have also been modelled using four-bar linkages and spatial parallel mechanisms [15, 25]. Parameter identification for a biaxial kinematic model for ankle joint has been investigated in an *in vivo* manner [23, 26]. However, in the present research, we have further extended this work and used it in the larger musculoskeletal ankle model. In order to study passive and active behaviour of ankle complex, its overall moment-displacement relationship had been studied [2, 27-34], however, active ankle behaviour in transverse and frontal planes has not been reported. While some models treated the bones as rigid bodies and ignored effects caused by deformation of soft tissues [9, 19, 20, 22], others applied computationally expensive finite element analysis on the bones and soft tissue in order to obtain the stress distribution across the articulating bone surfaces [7, 8, 35, 36]. Effects of ligaments on the ankle complex biomechanics had also been considered by treating them as tension only elastic elements [7-9, 37]. Most of these, however, include the influence of ligaments on passive joint stiffness as a lumped effect[19, 20]. Properties of muscles and tendons are also commonly included in such models by researchers [19, 20, 22]. There are few other instances [38, 39] wherein numerical models are used to assess muscle behaviours for their intended purpose.

This study aims to develop a musculoskeletal model of the ankle complex to facilitate measurement of passive and active ankle complex motions and moments. The ankle musculoskeletal model has constituent biomechanical model of the ankle complex and viscoelastic models of ligaments and muscle-tendon units. Each of these constituent models is further discussed in detail in the following sections. According to authors' best knowledge, ankle complex modelling (to estimate joint moments) in three anatomical axes and its validation has not been reported in literature.

II. METHODS

A. *Musculoskeletal ankle modelling*

Kinematic model of the ankle complex

The kinematics related to the biaxial ankle model can be devised using homogeneous transformation matrices. In order to transform a point expressed in frame B to its equivalent representation in frame A, the orientation and translation of frame B relative to frame A is considered. Use of homogeneous transformation matrix can be further expressed by (1), where $T_{AB} \in \mathbb{R}^{4\times4}$ (2) is the homogeneous transformation matrix. Here, $R_{AB} \in \mathbb{R}^{3\times3}$ is the orthonormal matrix describing the orientation of frame B relating to

frame A, and $t_{AB} \in \mathbb{R}^3$ is the translation between origins of frame A&B (expressed in frame A). Similarly, $x_A, x_B \in \mathbb{R}^3$ are the respective locations of points relative to the origins of frame A&B, expressed in frame A&B coordinates. These variables are also explained with the help of a diagram shown in Figure 1a. Inverse of a homogeneous transformation matrix exists and can be represented by (3).

$$\begin{bmatrix} x_A \\ 1 \end{bmatrix} = T_{AB} \begin{bmatrix} x_B \\ 1 \end{bmatrix} \quad (1)$$

$$T_{AB} = \begin{bmatrix} R_{AB} & t_{AB} \\ 0_{1\times3} & 1 \end{bmatrix} \quad (2)$$

$$T_{AB}{}^{-1} = T_{BA} = \begin{bmatrix} R_{AB}{}^{T} & -R_{AB}{}^{T} t_{AB} \\ 0_{1\times3} & 1 \end{bmatrix} \quad (3)$$

Figure 1: **(a)** Pictorial presentation of variables used in (**1**-**3**), **(b)** Additional degrees of freedom in the 16-parameter kinematic model compared to the 12-parameter model.

Next, the ankle, subtalar and foot coordinate frames can be defined with respect to a fixed global frame. The subtalar frame was considered to be fixed on the talus but its orientation can change via rotation about the subtalar joint. On the other hand, the ankle frame was taken to be fixed on the tibia and is free to rotate about the ankle joint axis. Ankle frame (A) orientation with respect to the global coordinates can be obtained by consecutive rotations about the *y* and *z* axes of the global frame. Likewise, the subtalar frame (S) can be obtained by applying *y* and *z* rotations about the ankle frame. Three translations are also required to reposition individual frame's origins at designated points in the global frame. A total of five parameters were therefore required to define each of the ankle and subtalar frames while the foot is at its neutral position.

Apparently, the homogeneous transformation matrices for the ankle, subtalar and foot coordinate frames at the neutral foot position can be given by (4-6), where R_z and R_y are the rotational transformation matrices about the *z* and *y* axes respectively, and subscripts, a, s and f related to the ankle, subtalar and foot coordinate frames. It is important to mention here that subscript i refers the neutral foot position of a variable.

$$T_{0a,i} = \begin{bmatrix} R_{0a,i} & t_{0a} \\ 0_{1\times3} & 1 \end{bmatrix} = \begin{bmatrix} R_{z,a}R_{y,a} & t_{0a} \\ 0_{1\times3} & 1 \end{bmatrix} \quad (4)$$

$$T_{0s,i} = T_{0a,i}T_{as,i} = T_{0a,i} \begin{bmatrix} R_{as,i} & t_{as,i} \\ 0_{1\times3} & 1 \end{bmatrix} = T_{0a,i} \begin{bmatrix} R_{z,s}R_{y,s} & t_{as,i} \\ 0_{1\times3} & 1 \end{bmatrix} \quad (5)$$

$$T_{0f,i} = \begin{bmatrix} R_{0f,i} & t_{0a} \\ 0_{1\times3} & 1 \end{bmatrix} = \begin{bmatrix} I_3 & t_{0f,i} \\ 0_{1\times3} & 1 \end{bmatrix} \quad (6)$$

The final homogeneous transformation matrix associated with the foot frame can now be obtained as shown in (7). Here, R_x represents the transformation matrix for *x*-axis rotations.

$$T_{0f} = T_{0a,i} \begin{bmatrix} R_{x,a} & 0_{3\times1} \\ 0_{1\times3} & 1 \end{bmatrix} T_{0a,i}{}^{-1} T_{0s,i} \begin{bmatrix} R_{x,s} & 0_{3\times1} \\ 0_{1\times3} & 1 \end{bmatrix} T_{0s,i}{}^{-1} T_{0f,i} \quad (7)$$

The model formulated here has 16 parameters, whereby six parameters are required to define $T_{0f,i}$ when the orientation of the neutral foot frame is arbitrary. On the other hand, the models proposed by [23, 40] use only 12 parameters meaning that the proposed model may not be the minimal realisation of the biaxial model. Nevertheless, two of the four additional parameters are the angular offsets needed at each revolute joint to nullify the ankle and subtalar joint displacements at the neutral foot orientation. The remaining two parameters on the other hand are for positions of the origins of the ankle and subtalar frame which can be varied along the corresponding revolute axis (as illustrated in Figure 1b). Therefore, in the proposed model, there is an additional degree of freedom available

for locating each of these origins along their respective axes. The present model, with16 parameters, is obviously an improvement from the previous models.

B. Characterization of Musculoskeletal Elements of the Ankle Joint

Viscoelastic Characterization of Ligaments:

The medial and lateral ligaments are soft tissues connecting articulating bone segments and can be considered as linear viscoelastic materials. Force response of such materials for a step strain input is normally given by a relaxation function $G(t)$ which can be further used to calculate the force response over an arbitrary strain history [41].

Figure 2: (a) Ankle ligament represented by spring-dashpot model, (b) Viscoelastic model of the muscle-tendon unit.

This behaviour can also be emulated using a linear viscoelastic model represented by a linear arrangement of springs and dampers or dashpots. In order to illustrate the force-relaxation behaviour of ligaments, a generalized Maxwell model for a step displacement x is shown in the Figure 2a. Here elastic behaviour is modelled using a simple spring (k) whereas to model viscoelastic behaviour, an array of serial combination of springs and dashpots is considered.

Amongst several other linear viscoelastic models, the model proposed by Funk *et al.* [41] for the quantification of viscoelasticity of ankle ligaments is more suitable for the present research owing to its simplicity. Without the loss of generality, a linear version of this model which is Maxwell's model [42] can be used whereby three spring-dashpot units in parallel with another spring (k) are employed to model ligament characteristics. Further, to reduce model complexity in the present work, one pair of spring-dashpot unit in parallel to a spring element has been chosen to approximate the ligament behaviour resulting less than 10% mean error in the strain produced. Going back to the Funk's model, ligament forces can be assumed having two components, a steady state force along spring element to account for the strain and the serial spring dashpot unit for the time dependent component of the ligament forces. The ligament force thus can be found by simply summing up these two force components (8).

$$F_{lig} = F_e(x_0) + F_d(x_1) \tag{8}$$

$$F_{lig} = k_0 x_0 + (k_1 x_1 + c_1 \dot{x}_{1d}) \tag{9}$$

$$x_0 = x_1 + x_{1d};\ \ or\ \ x_{1d} = x_0 - x_1 \tag{10}$$

$$\dot{x}_{1d} = \dot{x}_0 - \frac{1}{c_1} F_d(x_1) \tag{11}$$

Here x_0 is the deflection along single spring, whereas x_1 is the effective elongation produced in the spring-dashpot unit. The dashpot is assumed to be having a linear elongation (x_{1d}) with c_1 as its damping coefficient. Referring back to Funk's model, the elastic response, which is further a linear function of strain, can be modelled as (12).

$$F_e(x_0) = A_1(e^{B\frac{x_0}{L_0}} - 1) \tag{12}$$

The spring function in the model (12) is a function of strain where x_0 is the instantaneous displacement and L_0 is the relaxed length of the subject ligament. Considering reduced relaxation function coefficient $G(t)$, this function can also be further improved as (13) making spring parameters as nonlinear functions of elongation.

$$F_e(x_0) = G_i(t)\, A_1(e^{B\frac{x_0}{L_0}} - 1) \tag{13}$$

The dashpot function can also be modified in order to make time constants independent of strain.

$$c_i(x) = k_i . t_i \tag{14}$$

The above quasi-linear model was linearized by applying these equations at a reference displacement (10% strain level) and subsequently spring and dashpot functions (c_i, k_i) were obtained and used in (8-11). Apparently, the ligament force increases exponentially with the strain and at higher values, small increment in strain may result in very high force values which should be avoided looking to the fibre strength of ligaments. Therefore, in the present work, referring to the maximum failure load a muscle can take, we have capped the force value at a limiting value of 700N. Force and strain relation for the ligaments obtained from the linear visco-elastic model seem to be in agreement with their corresponding experimental findings (Figure 3a).

Characterization of Muscle-tendon units:

Muscles, by virtue of their fibrous structure, can generate forces and cause movements. Similarly, tendons are also made of fibers and behave as a link between bones and muscles to transfer the muscle force to the skeletal joints. While tendons can be modeled as passive elastic elements, muscles are difficult to model owing to their complex dynamics and force generating capacity. Nevertheless, for the present work we have used the existing Hill based model [19, 20, 43, 44] to model muscles. Tendons are modelled with non-linear springs and the muscles are assumed to be made up of two components i.e. an active contractile element (CE) and a passive element (PE) connected in parallel to CE. In order to represent passive muscle behaviour, PE consists of a nonlinear spring (K_{PE}) and a dashpot (C_{PE}) as shown in Figure 2b. Line of action for the muscle force is normally not aligned along the muscle and therefore a pennation angle θ is used for the angle between direction of force and muscle-tendon unit alignment.

Force along the contractile element (F_{CE}) is a function of strain (ε) as well as strain rate ($\dot{\varepsilon}$) and can be typically given by (15). Here A is an activation function of muscles which has values between zero and unity and is a measure of the extent of muscle force realized. The maximum muscle force is denoted by $F_{\max}$ in the following formulations. The contractile force can also be termed as a function of force-length and force-velocity relations, where $f_l = -k\varepsilon$ and $f_v = -c\dot{\varepsilon}$.

$$F_{CE}(A, \varepsilon, \dot{\varepsilon}) = (AF_{\max}) f_l(\varepsilon) f_v(\dot{\varepsilon}) \tag{15}$$

Further, working with tendon and PEs, their force-length relationships is normally approximated extracting information from software packages such as PyODE and Opensim [45, 46]. In the present work, we have referred Opensim and developed f_l and f_v functions by considering various data points and developing cubic spline interpolation. These functions are illustrated in Figure 3c, wherein, lengths of CE have been normalized assuming lengths of muscle fibre to be maximum at the time the muscle active force is maximum. On the other hand, force-velocity relation can be formulated mathematically as (16) where, a_f is a scalier factor which depends on the manner, (fast and slow) twitch fibres are composed in the muscle also $\dot{\varepsilon}$ stands for the normalized strain rate in the contractile element. In order to define the force-velocity relationship when the muscle stretch velocity is positive, α and β parameters are used which are material constants. These parameters help in providing a desired limiting value for $f_v(v_{CE})$ when the muscle velocity approaches infinity or very high values (Figure 3c). In terms of actuation, the normalized strain rate $\dot{\varepsilon}$ can be taken as $\frac{v_{CE}}{|v_{max}|}$, where v_{max} is the maximum contraction speed of the muscle being considered.

$$f_v(v_{CE}) = \begin{cases} \frac{a_f(1+\dot{\varepsilon})}{(a_f-\dot{\varepsilon})} & duirng\ isotonic\ contraction \\ \frac{1+\alpha\dot{\varepsilon}}{1+\beta\dot{\varepsilon}} & during\ extension \end{cases} \tag{16}$$

Subsequent to the above formulations, a state space model was developed to solve the dynamics of the muscle-tendon unit, considering length of the contractile element as the state variable. Further, lengths and forces of various components were modelled as shown in (17) and (18), where l_{mt} is the total length of the muscle-tendon unit and F_{MT} is the force along the muscle-tendon unit. As a matter of fact, the force experienced by the tendon is same as force generated at the muscle unit. Here force along the tendon F_T and force along the parallel element F_{PE} are represented by (19) and (20) respectively.

Figure 3: (a) Nonlinear Viscoelastic behaviour from model against experimental data, (b) The moment-angular displacement relationship generated by applying a slow moment ramp input to the developed ankle model (c) Normalised force and its relationship with strain and rate of strain for tendon, PE & CE element in Hill type model.

$$l_{mt} = l_t + l_{ce}\cos\theta \tag{17}$$

$$F_{MT} = F_T = (F_{CE} + F_{PE})\cos\theta \tag{18}$$

$$F_T = AF_{max}(e^{B_1\varepsilon} - 1) \tag{19}$$

$$F_{PE} = AF_{max}(e^{B_2\varepsilon} - 1) + c_{pe}v_{ce} \tag{20}$$

Using simple procedures, equations (20) and (17-20) leads to (21), which describes the time-based actuation of the contractile element with muscle activation and current length of the muscle-tendon unit. Definite solution for v_{ce} can be found by first expanding (21) into a quadratic function (22) and then finding the roots of the equation by appropriately selecting solutions considering their sign. However, it should be noted that obtaining v_{CE} using (21) will not be sufficient since this quantity is also used to obtain the active segment of the function (21). Therefore, in this work we have taken into account the fact that $f_v(v_{CE})$ is greater than unity while muscle is extending and less than unity when the muscle is contracting. Furthermore, other parameters such as A, F_{max}, f_{pe} and f_{ce} are all positive by definition, the tendon force will be greater than the static component of the muscle force, as shown in (23), provided v_{CE} is positive and vice versa. Thus in order to obtain the sign of v_{CE} this force difference can be used while selecting the appropriate segment of (21) to be used in (22).

$$F_{max}f_t(l_{mt} - l_{ce}\cos\theta) = \left[AF_{max}f_l(\varepsilon)f_v(\dot{\varepsilon}) + AF_{max}(e^{B_2\varepsilon} - 1) + c_{pe}v_{ce}\right]\cos\theta \tag{21}$$

$$AF_{max}(e^{B_1\varepsilon} - 1) - \left[AF_{max}(e^{B_2\varepsilon} - 1) + c_{pe}v_{ce}\right]\cos\theta = \begin{cases} AF_{max}\cos\theta\,\frac{a_f(1+\dot{\varepsilon})}{(a_f - \dot{\varepsilon})} & \bar{F} < 0 \\ AF_{max}\cos\theta\,\frac{1+\alpha\dot{\varepsilon}}{1+\beta\dot{\varepsilon}} & \bar{F} \geq 0 \end{cases} \tag{22}$$

$$\bar{F} = AF_{max}(e^{B_1\varepsilon} - 1) - AF_{max}[f_l(\varepsilon) + (e^{B_2\varepsilon} - 1)]\cos\theta = AF_{max}[f_v v_{ce} - 1]f_l(\varepsilon)\cos\theta + c_{pe}v_{ce}\cos\theta \tag{23}$$

C. Model Implementation

Two main factors that influence the length of ligaments and muscle-tendon units are locations of the origin and insertion points for the force element**.** In the proposed model the ankle and subtalar joint displacements are considered as state variables while insertion and origin points of force elements represent variables.

Table 1: Ligaments at the ankle, subtalar joints and foot muscles considered during the ankle model development

It should be noted here that only main muscle-tendon units and ligaments (listed in the Table 1), which span ankle & subtalar joints, are considered during modelling. Further, the attachment sites are treated as points and the force elements are modelled as lines. A

graphical user interface (GUI) [47] had been developed in MATLAB to facilitate the conversion of visual information to quantitative data utilizing a three-dimensional surface model of the entire lower limb skeleton [48]. The GUI can also be used to identify force relationship parameters of these elements. The force-strain parameters for ligaments used in this work are in agreement to those mentioned in [49], whereas the parameters related to muscles were same as in [22, 50]. Later, the location information and force parameters are finally used in the overall ankle model.

The surface model data is given as a three-dimensional point cloud input with a connectivity matrix which maps the relation between these points to form the bone surface. Later, axes representing the ankle and subtalar joints were defined before determining the force element attachment points and subsequently the joint coordinate frames were defined. Later, the attachment points for the ligaments and tendons were obtained by selecting these attachment sites of the force elements available in the anatomical resources [22, 51]. Subsequently, a rendered bone surface plot was created using these attachment points. Points on the talus were expressed in the ankle joint coordinate frame and similarly points on the other foot bones were mapped in the subtalar joint coordinates. All points connected to the tibia and fibula bones were expressed in the global dataset coordinate frame.

Force elements such as muscle-tendon units, cannot be assumed to be having straight paths, since they normally wrap around various bones and ligaments. Therefore, this wrapping characteristics is vital to understand to produce more pragmatic simulations and their feasible results. In the present work, the muscle path is made to pass though certain intermediate points before finally joining the insertion point. In order to determine length of each force element, suitable equations (24,25) can be used where l_k is the length of the force element, n_k is the total number of attachment points, i is an index representing the attachment point being considered, $F_i = O, A, S$ is an identifier for the joint coordinate frame which corresponds to the i^{th} attachment point (where O, A and S are respectively used to denote the dataset frame, the ankle frame and the subtalar frame), T_{0F_i} is the homogeneous transformation matrix which transform the dataset coordinate frame to the corresponding joint coordinate frame; and $P_{k,F_i,i}$ is the position vector of the attachment point i for the k^{th} force element, expressed in the local coordinates of the F_i frame.

$$l_k = \sum_{i=1}^{i=n_k-1} \left\| v_{i,i+1} \right\| \quad (24)$$

$$v_{i,i+1} = [I_3 \quad 0_{3\times1}]\left(T_{0F_{i+1}} P_{k,F_{i+1},i+1} - T_{0F_i} P_{k,F_i,i}\right) \quad (25)$$

III. Results

Model Validation

Ankle Model Validation with Previous Work

In order to validate, the developed ankle model required to be evaluated against experimental studies. However, the moments and displacement data from experiments performed on subjects is likely to vary considerably between subjects and as such we do not expect accurate and complete agreement during such comparison. Therefore, it would be more appropriate here to discuss whether the developed model qualitatively approximates the observations on real human ankle complex motions.

The validation was carried out for two kinds of ankle motions namely, passive and active ankle motions. In order to obtain active muscle behaviour from the model, muscle activation profiles related to the flexion and inversion-eversion moments were given as input to the model and the response of the ankle model was recorded and compared with the requisite trajectories.

Finally, the model was also compared with data obtained from an unactuated (passive) parallel ankle robot [4], used by three healthy subjects through flexion and inversion-eversion trajectories.

Passive Moment-Displacement Characteristics

In order to carry out experiments to assess the ankle model for the passive moment-displacement relationships under static conditions, a ramp input of external moment is applied about the *x*-axis i.e. in the flexion direction. The results from the model (Figure 3b) are in close agreement with typical ankle moment-displacement relations found in the literature [2]. Values for ankle moments were small around the neutral foot position which gradually increased rather rapidly when the foot moved towards extremities. Further, higher stiffness and smaller motion range was observed in the dorsiflexion direction compared to those in the plantarflexion direction which further is an endorsement of the previous works and results published by Riener and Edrich [2]. The range of ankle motions from simulations (Figure 3b) was also found to be in agreement with the experimental results e.g. larger range of motions was observed in the inversion direction as compared to the eversion motion.

Active Ankle-Complex Behaviour

While validating the proposed model in predicting the active ankle motions, experiments were performed by actuating certain group of leg muscles and analysing the resulting ankle motions. Six cases were considered and the resulting motions in terms of XYZ Euler angles are displayed in Figure 4. Here, *case A* represents the activation of plantarflexor muscles, *case B* shows the dorsiflexor muscles activation and resulting motion, *case C* involves the invertor muscles' group, *case D* shows the motion resulting dorsiflexor and evertor muscles' actuation. Likewise, *case E* involves adduction muscles and *case F* illustrates motion involving abduction muscles.

In order to realize muscle activation signals, a step activation is passed through a low pass filter prior to applying this in the dynamic equations of the muscle-tendon units. Results from simulations show that the model responses largely agreed with the expected foot behaviour, since the activation of the muscles had produced the desired foot motion.

Figure 4: Time histories of the foot orientation in XYZ Euler angles obtained from simulations of the developed ankle model with muscle activations.

Information about the forces along the ankle ligaments is important during ankle joint rehabilitation treatments. Subject specific rehabilitation trajectories can be selected in such a manner that the weak ligaments are not subjected to higher forces. Therefore, during another set of experiments (active mode), ligament forces were measured during ankle supination trajectory (Figure 5). The group of muscles for which forces were recorded was found to be the one responsible for the ankle supination trajectory.

Figure 5: Magnitudes of ligament tensions during supination trajectory (ATaFL: Anterior TaloFibular Ligament; CFL: Calcaneofibular Ligament; LTaCL: Lateral Talocalcaneal Ligament; PTaFL: Posterior TaloFibular Ligament)

Experimental Validation of Ankle Model

Finally the ankle model was also compared with the findings from experimental trials involving the ankle rehabilitation robot [4]. During these experiments the ankle robot was used with three healthy subjects along certain trajectories. Appropriate ethics approval

was obtained and subjects were asked to remain relaxed during these trials. Force data from the load cells is extracted along with the actuator length data. While, actuator force data was converted to moments (using platform geometry of the ankle robot), the actuator length data was converted to foot orientations. Later, these moments were applied to the musculoskeletal ankle model and the resulting Euler angles from the model foot were compared with the experimentally recorded foot Euler angles (Figure 6). Related ankle motion trajectories obtained from the ankle robot were also plotted simultaneously for a quick comparison.

Figure 6: (a) Comparison of foot orientations (XYZ Euler angles) obtained from the ankle robot (blue) and foot orientation from the model (red). (b) Moment information extracted from actuator force data.

IV. Discussion

During validation, the proposed ankle model was used in two modes, namely, passive and active modes. Results from the model during passive mode were found to be in close agreement with those established by previous researches (Figure 3b). However, in order to evaluate the ankle model in active mode, six scenarios were evaluated whereby groups of muscles responsible for a certain trajectory were activated and the resulting trajectories were analyzed (Figure 4). In yet another experiment with the model during active mode, ligament forces were measured during ankle supination trajectory (Figure 5). It was found that the group of active muscles was same as the group of muscles responsible for the ankle supination trajectory.

During experimental trials with the ankle rehabilitation robot (Figure 6), the values of Euler angles were of the same order of magnitude and had a quite similar profile in both the trajectories. Small discrepancies in the X and Y Euler angles observed during start of the simulations were mainly due to the friction in actuator connections on the ankle robot. Deviations for the Z Euler angle displacement can be attributed to the differences in kinematic constraints between the subject and the model. While there are experimental errors and the model is of non-subject specific nature, observance of qualitative agreement between the model and experimental data is encouraging.

An important aspect of the proposed ankle model is that the functions of individual ligaments and muscle-tendon units are being investigated instead of lumping these into a single resistive moment-joint displacement relationship. This information can be used to provide an indication of the forces along such force elements and to analyze effects of different motion trajectories on tensions in these force elements. Apart from using this model in robot controller simulation, it can also be effectively used to evaluate rehabilitation trajectories. Future work in this research shall be carried out to investigate suitability of different rehabilitation trajectories by evaluating the force element tensions and joint reaction moments associated with them.

V. Conclusion

A musculoskeletal ankle model was developed taking human ankle as a combination of ankle joint and subtalar joint. Biomechanical characteristics of bone joints, ligaments and muscle-tendon elements were studied and modeled while developing the ankle model. The resulting model is a multi-rigid body model and incorporation of ligaments and muscle-tendon units allowed this model to be used to study the effects of different motion trajectories on the force elements. Such information is crucial in the study of multi joint

mechanics of human motions and can be used during physical treatments of lower limb impairment. Musculoskeletal information from the ankle model can also be used to develop rehabilitation robots or assess performance of existing robots. Such models also find their application in the development of rehabilitation trajectories necessary for subject specific treatments.

The main contribution of this research is in estimating the joint moments in three anatomical axes of ankle joint and quantifying the tensions in force elements around the ankle joint. Ankle joint modelling (to estimate passive and active joint moments) in three anatomical axes along with appropriate validation has not been reported in the literature and therefore the proposed model may be helpful in quantifying ankle joint functions while assessing ankle injuries.

REFERENCES

1. Edrich, T., R. Riener, and J. Quintern, *Analysis of passive elastic joint moments in paraplegics.* IEEE Transactions on Biomedical Engineering, 2000. **47**(8): p. 1058-1065.
2. Riener, R. and T. Edrich, *Identification of passive elastic joint moments in the lower extremities.* Journal of Biomechanics, 1999. **32**(5): p. 539-544.
3. Lee, H., et al., *Multivariable static ankle mechanical impedance with active muscles.* IEEE Transactions on Neural Systems and Rehabilitation Engineering, 2014. **22**(1): p. 44-52.
4. Jamwal, P.K., et al., *An Adaptive Wearable Parallel Robot for the Treatment of Ankle Injuries.* Mechatronics, IEEE/ASME Transactions on, 2014. **19**: p. 64-75.
5. Tsoi, Y.H., S.Q. Xie, and G.D. Mallinson. *Joint force control of parallel robot for ankle rehabilitation*. in *2009 IEEE International Conference on Control and Automation, ICCA 2009*. 2009.
6. Cheung, J.T.-M. and B.M. Nigg, *Clinical applications of computational simulation of foot and ankle.* Sports Orthopaedics and Traumatology, 2008. **23**(4): p. 264-271.
7. Cheung, J.T.-M., M. Zhang, and K.-N. An, *Effects of plantar fascia stiffness on the biomechanical responses of the ankle-foot complex.* Clinical Biomechanics, 2004. **19**(8): p. 839-846.
8. Cheung, J.T.-M., et al., *Three dimensional finite element analysis of the foot during standing - a material sensitivity study.* Journal of Biomechanics, 2005. **38**: p. 1045-1054.
9. Liacouras, P.C. and J.S. Wayne, *Computational modeling to predict mechanical function of joints: Application to the lower leg with simulation of two cadaver studies.* Journal of Biomechanical Engineering, 2007. **129**: p. 811-817.
10. Barnett, C.H. and J.R. Napier, *The axis of rotation at the ankle joint in man; its influence upon the form of the talus and the mobility of the fibula.* Journal of Anatomy, 1952. **86**(1): p. 1-9.
11. Lundberg, A., et al., *The axis of rotation of the ankle joint.* Journal of Bone and Joint Surgery - Series B, 1989. **71**(1): p. 94-99.
12. Engsberg, J.R., *A biomechanical analysis of the talocalcaneal joint - in vitro.* Journal of Biomechanics, 1987. **20**(4): p. 429-442.
13. Demarais, D.M., R.A. Bachschmidt, and G.F. Harris, *The instantaneous axis of rotation (IAOR) of the foot and ankle: A self-determining system with implications for rehabilitation medicine application.* IEEE Transactions on Neural Systems and Rehabilitation Engineering, 2002. **10**(4): p. 232-238.
14. Ying, N. and W. Kim, *Determining dual Euler angles of the ankle complex in vivo using "flock of birds" electromagnetic tracking device.* Journal of Biomechanical Engineering, 2005. **127**: p. 98-107.
15. Leardini, A., et al., *A geometric model of the human ankle joint.* Journal of Biomechanics, 1999. **32**: p. 585-591.
16. Dettwyler, M., et al., *Modelling of the ankle joint complex. Reflections with regards to ankle prostheses.* Foot and Ankle Surgery, 2004. **10**: p. 109-119.
17. Apkarian, J., S. Naumann, and B. Cairns, *A three-dimensional kinematic and dynamic model of the lower limb.* Journal of Biomechanics, 1989. **22**(2): p. 143-155.
18. Dul, J. and G.E. Johnson, *A kinematic model of the human ankle.* Journal of Biomedical Engineering, 1985. **7**: p. 137-143.
19. Wright, I.C., et al., *The influence of foot positioning on ankle sprains.* Journal of Biomechanics, 2000. **33**: p. 513-519.
20. Wright, I.C., et al., *The effects of ankle compliance and flexibility on ankle sprains.* Medicine & Science in Sports & Exercise, 2000. **32**(3): p. 260-265.
21. Scott, S.H. and D.A. Winter, *Biomechanical model of the human foot: kinematics and kinetics during the stance phase of walking.* Journal of Biomechanics, 1993. **26**(9): p. 1091-1104.
22. Delp, S.L., et al., *OpenSim: Open-source software to create and analyze dynamic simulations of movement.* IEEE Transactions on Biomedical Engineering, 2007. **54**(11): p. 1940-1950.
23. van den Bogert, A.J., G.D. Smith, and B.M. Nigg, *In vivo determination of the anatomical axes of the ankle joint complex: an optimization approach.* Journal of Biomechanics, 1994. **27**(12): p. 1477-1488.
24. Inman, V.T., *The joints of the ankle*. 1976, Baltimore: Williams and Wilkins.
25. Gregorio, R.D., et al., *Mathematical models of passive motion at the human ankle joint by equivalent spatial parallel mechanisms.* Medical and Biological Engineering and Computing, 2007. **45**: p. 305-313.
26. Lewis, G.S., H.J. Sommer Iii, and S.J. Piazza, *In vitro assessment of a motion-based optimization method for locating the talocrural and subtalar joint axes.* Journal of Biomechanical Engineering, 2006. **128**(4): p. 596-603.
27. Silder, A., et al., *Identification of passive elastic joint moment-angle relationships in the lower extremity.* Journal of Biomechanics, 2007. **40**(12): p. 2628-2635.
28. Kearney, R.E., P.L. Weiss, and R. Morier, *System identification of human ankle dynamics: intersubject variability and intrasubject reliability.* Clinical Biomechanics, 1990. **5**: p. 205-217.

29. Riener, R. and T. Edrich, *Identification of passive elastic joint moments in the lower extremities.* Journal of Biomechanics, 1999. **32**: p. 539-544.
30. Hunter, I.W. and R.E. Kearney, *Dynamics of human ankle stiffness: Variation with mean ankle torque.* Journal of Biomechanics, 1982. **15**(10): p. 747-752.
31. Kearney, R.E. and I.W. Hunter, *Dynamics of human ankle stiffness: Variation with displacement amplitude.* Journal of Biomechanics, 1982. **15**(10): p. 753-756.
32. Parenteau, C.S., D.C. Viano, and P.Y. Petit, *Biomechanical properties of human cadaveric ankle-subtalar joints in quasi-static loading.* Journal of Biomechanical Engineering, 1998. **120**: p. 105-111.
33. Chen, J., S. Siegler, and C.D. Schneck, *The three-dimensional kinematics and flexibility characteristics of the human ankle and subtalar joint- Part II: Flexibility characteristics.* Journal of Biomechanical Engineering, 1988. **110**: p. 374-385.
34. Piazza, S.J. and G.S. Lewis, *Computational models of the foot and ankle.* Current Opinion in Orthopaedics, 2003. **14**: p. 79-83.
35. Giddings, V.L., et al., *Calcaneal loading during walking and running.* Medicine & Science in Sports & Exercise, 2000. **32**(3): p. 627-634.
36. Fontanella, C.G., et al., *Biomechanical behavior of plantar fat pad in healthy and degenerative foot conditions.* Medical and Biological Engineering and Computing, 2015.
37. Haraguchi, N., et al., *Prediction of three-dimensional contact stress and ligament tension in the ankle during stance determined from computational modeling.* Foot & Ankle International, 2009. **30**(2): p. 177-185.
38. Ghiasi, M.S., et al., *Investigation of trunk muscle activities during lifting using a multi-objective optimization-based model and intelligent optimization algorithms.* Medical and Biological Engineering and Computing, 2015.
39. Pavan, P.G., et al., *Biomechanical behavior of human crural fascia in anterior and posterior regions of the lower limb.* Medical and Biological Engineering and Computing, 2015.
40. Lewis, G.S., H.J. Sommer, and S.J. Piazza, *In vitro assessment of a motion-based optimization method for locating the talocrural and subtalar joint axes.* Journal of Biomechanical Engineering, 2006. **128**: p. 596-603.
41. Funk, J.R., et al., *Linear and quasi-linear viscoelastic characterization of ankle ligaments.* Journal of Biomechanical Engineering, 2000. **122**(1): p. 15-22.
42. Myers, B.S., J.H. McElhaney, and B.J. Doherty, *The viscoelastic responses of the human cervical spine in torsion: Experimental limitations of quasi-linear theory, and a method for reducing these effects.* Journal of Biomechanics, 1991. **24**(9): p. 811-817.
43. Winters, J.M., *Hill-based muscle models: A system engineering perspective*, in *Multiple Muscle Systems: Biomechanics and Movement Organization*, J.M. Winters and S.L.-Y. Woo, Editors. 1990, Springer-Verlag: New York. p. 69-91.
44. Yamada, H. and J. Kajzer, *A mathematical model of skeletal muscle and numerical simulations of its response under stretching.* JSME International Journal, Series C: Mechanical Systems, Machine Elements and Manufacturing, 1999. **42**(3): p. 508-513.
45. Awa, Y. and K. Kobayashi. *Kinematics simulation by using ODE and MATLAB*. in *Proceedings of the SICE Annual Conference*. 2007.
46. Delp, S.L., et al., *OpenSim: Open-Source Software to Create and Analyze Dynamic Simulations of Movement.* Biomedical Engineering, IEEE Transactions on, 2007. **54**(11): p. 1940-1950.
47. Fenfang, Z., et al. *A computational biomechanical model of the human ankle for development of an ankle rehabilitation robot*. in *MESA 2014 - 10th IEEE/ASME International Conference on Mechatronic and Embedded Systems and Applications, Conference Proceedings*. 2014.
48. Virtual Animation of the Kinematics of the Human for Industrial Educational and Research purposes (VAKHUM). *VAKHUM public dataset.* July 14]; Available from: http://www.ulb.ac.be/project/vakhum/public_dataset/public-data.htm.
49. Funk, J.R., et al., *Linear and quasi-linear viscoelastic characterization of ankle ligaments.* Journal of Biomechanical Engineering, 2000. **122**: p. 15-22.
50. Yamaguchi, G.T., et al., *A survey of human musculotendon actuator parameters*, in *Multiple Muscle Systems: Biomechanics and Movement Organization*, J.M. Winters and S.L.-Y. Woo, Editors. 1990, Springer-Verlag: New York.
51. Primal Pictures Ltd. *Primal Pictures Ltd*. Available from: www.anatomy.tv.

Table 1: Ligaments at the ankle, subtalar joints and foot muscles considered during the ankle model development

Ligaments		Muscles	
Ant. talofibular	Post. tibiotalar	Ext. digitorum longus	Peroneous longus
Calcaneofibular	Tibiocalcaneal	Extensor hallucis longus	Peroneous tertius
Interosseous talocalcaneal	Medial talocalcaneal	Flexor digitorum longus	Soleus
Lateral talocalcaneal	Anterior tibiotalar	Flexor hallucis longus	Tibialis anterior
Anterior talocalcaneal	Talonavicular	Gastrocnemius	Tibialis posterior
Posterior talofibular	Tibionavicular	Peroneous brevis	

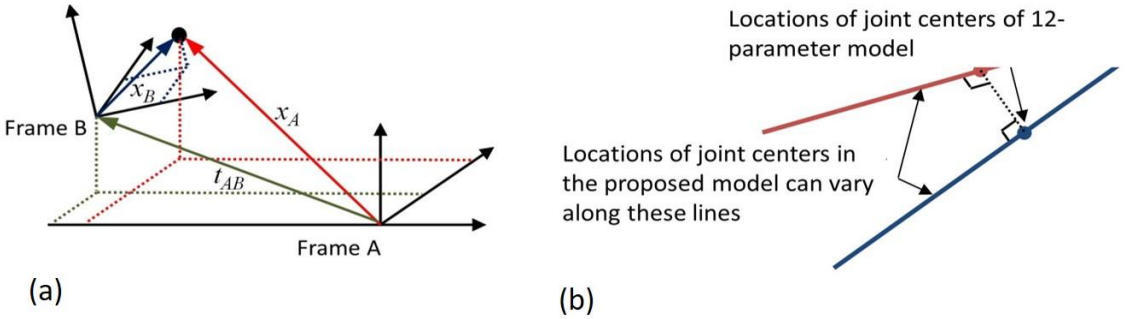

Figure 1: **(a)** Pictorial presentation of variables used in (**1**-**3**), **(b)** Additional degrees of freedom in the 16-parameter kinematic model compared to the 12-parameter model.

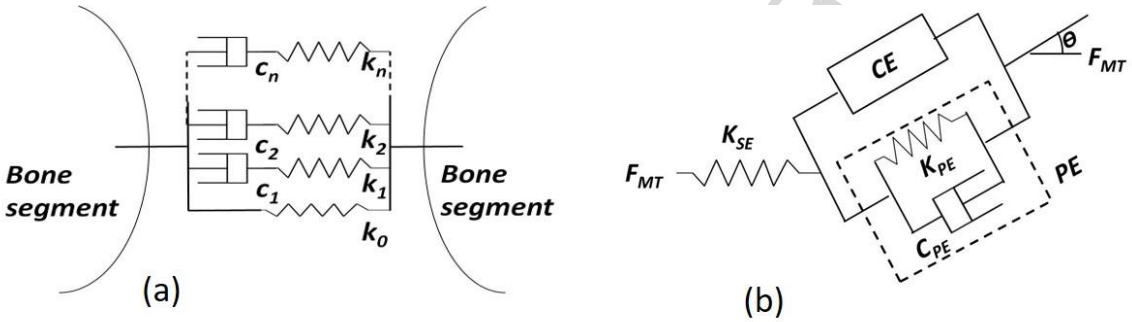

Figure 2: (a) Ankle ligament represented by spring-dashpot model, (b) Viscoelastic model of the muscle-tendon unit.

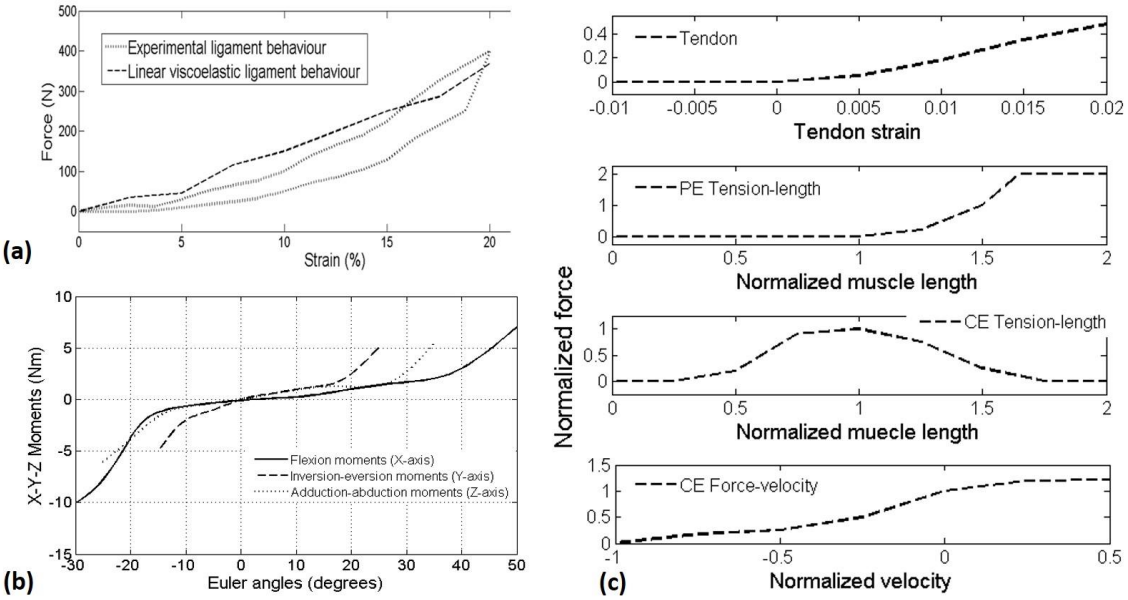

Figure 3: (a) Nonlinear Viscoelastic behaviour from model against experimental data, (b) The moment-angular displacement relationship generated by applying a slow moment ramp input to the developed ankle model (c) Normalised force and its relationship with strain and rate of strain for tendon, PE & CE element in Hill type model

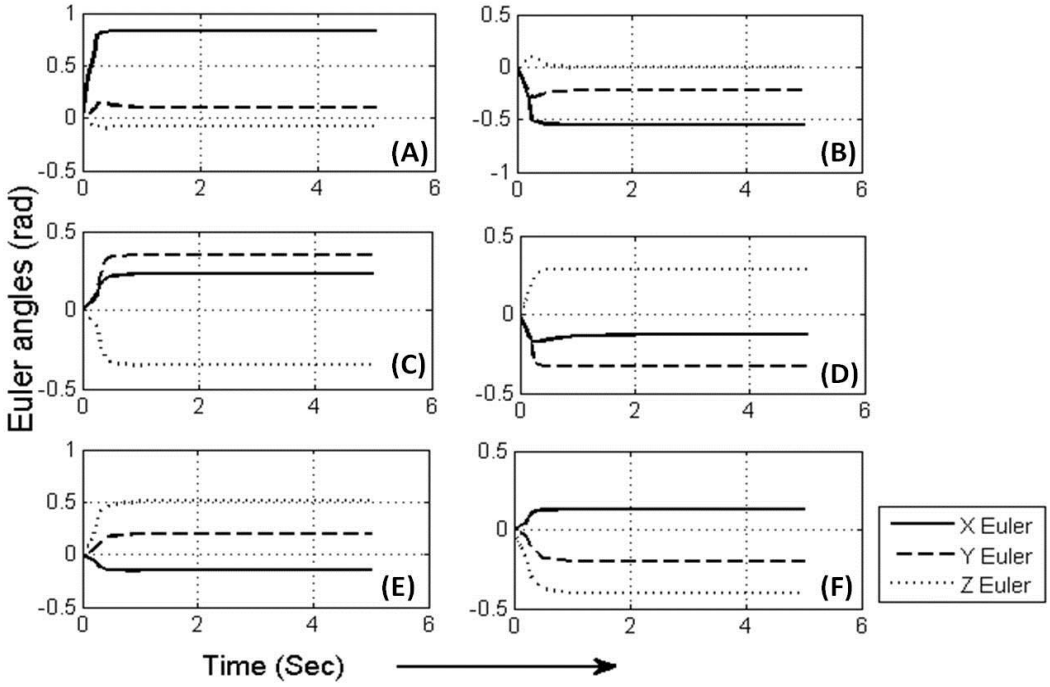

Figure 4: Time histories of the foot orientation in XYZ Euler angles obtained from simulations of the developed ankle model with muscle activations.

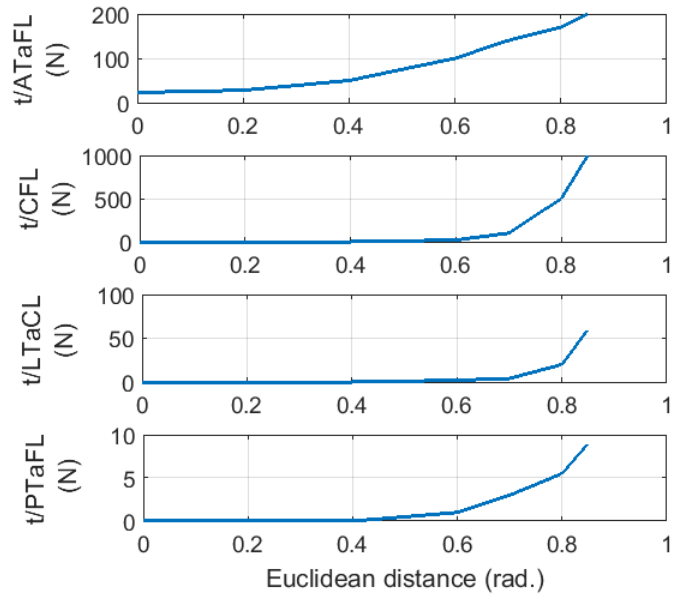

Figure 5: Magnitudes of ligament tensions during supination trajectory (ATaFL: Anterior TaloFibular Ligament; CFL: Calcaneofibular Ligament; LTaCL: Lateral Talocalcaneal Ligament; PTaFL: Posterior TaloFibular Ligament)

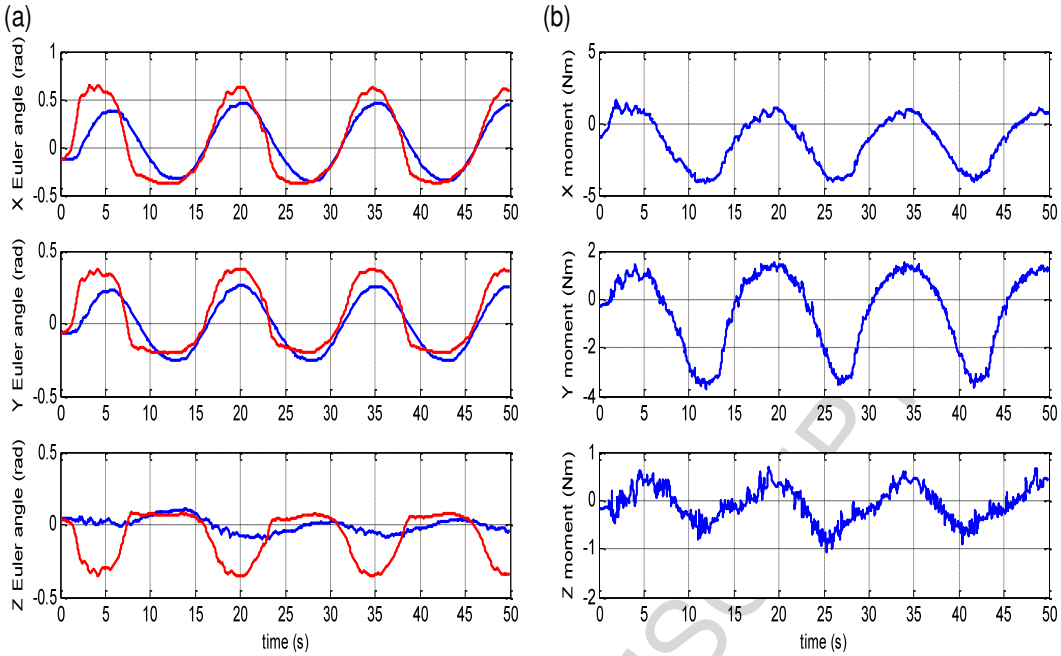

Figure 6: (a) Comparison of foot orientations (XYZ Euler angles) obtained from the ankle robot (blue) and foot orientation from the model (red). (b) Moment information extracted from actuator force data.

Highlights

- Musculoskeletal model of the ankle complex considering the biaxial structure.
- Model provides estimates of overall mechanical characteristics.
- Considerations of forces applied along ligaments and muscle-tendon units.
- Validation of the ankle model by comparing its outputs published literature
- Validation with experimental data from a parallel ankle rehabilitation robot.